**Egyptian Journal of Chemistry**

**http://ejchem.journals.ekb.eg/**

# Green cardamom mediated phytosynthesis of AuNPs and effect on the Activities of Nitric Oxide Synthase and 25-Hydroxyvitamin D 1-alpha-hydroxylase enzyme (CYP27B1) of Multiple sclerosis Patients

**Nada N. Ahmed [a], Salwa Hameed Naser Al-Rubae'i [a,*], and Waffa Mahdi Salih[b]**

[a] *Mustansiriyah University, College of Science, Department of Chemistry, Baghdad, Iraq.*
[b] *Mustansiriyah University, College of Science, Department of Physics, Baghdad, Iraq.*

**Abstract**

The development of pharmacotherapies that promote remyelination is a high priority for multiple sclerosis (MS), due to their potential for neuroprotection and restoration of function through repair of demyelinated lesions. A novel preparation of gold nanocrystals demonstrated robust remyelinating activity in response to demyelinating. The serum levels of NOS and CYP27B1enzyme for 90 MS patients and 30 controls were measured using enzyme-linked immune sorbent assay (ELISA). This project includes the green synthesis of gold nanoparticles using cardamom husks and a chemical reduction method. These methods resulted in pure spherical nanoparticles with small diameters of up to 20 nm without agglomerations. The nano-synthesized were investigated using X-ray diffraction (XRD), Photoluminescence (PL) and TEM. The toxicological effect of cardamom husks with gold nanoparticles AuNPs and AuNPs by chemical reduction on the growth of human neuroblastoma cell line (SH-SY5Y) cells was studied by examining the toxicity test (MTT) for 48 hours of exposure. The results showed that cardamom husks with gold nanoparticles AuNPs have the ability to inhibit the growth of SH-SY5Y cancer neuron cell lines, which proved effective at a concentration of 200 μmol/mL, as it achieved a killing rate of SH-SY5Y neurons at 46.644 % compared to the control group, which is the fibroblast cell line normal skin derived from human stem cells (HDFn), the toxicity rate was 19.637% for the presence of gold nanoparticles prepared using cardamom husks, while the toxicity for HDFn cells was 49.691% in the presence of gold nanoparticles prepared by the chemical method, which gives a clear inference that the method used for the synthesis of gold using cardamom husks achieved toxicity of 2.4 times less, which is considered a promising method for medical use. The work aimed to study the effects of nanoparticles on the levels of NOS and CYP27B1activity in the serum of newly diagnosed MS patients. The current study of AuNPs could be a stepping stone for future work to improve the binding between the vitamin D and its receptors inside the body and could be used to improve and modify a competitive ELISA method. These effects were the nanoparticles have an inhibition effect on the NOS synthase levels in sera of N-RRMS with MS patients. While the nanoparticles have not demonstrated effects inhibition on the binding between anti- CYP27B1antibody and antigen CYP27B1level in pool sera of MS patients.

**Keywords:** Green synthesis; Nanoparticles; Multiple sclerosis; SH-SY5Y Cell line; Demyelination;

## 1. Introduction

Multiple sclerosis (MS) is a chronic autoimmune inflammatory disease that causes demyelinating and degenerative lesions in the central nervous system (CNS). White matter axons ensure the passage of electrical signals in the nervous system [1, 2]. Myelin sheath surrounds a significant fraction of these axons, also known as nerve fibers. The myelin sheath's primary function is to increase the transmission speed along the axons, which is critical for long-distance communication. The central nervous system's myelin layer is attacked by immune cells in demyelinating illnesses, including multiple sclerosis [3, 4, 5]. The exact etiology of MS is unclear but complex interactions between genetic and environmental factors are considered involved in the autoimmune inflammatory process [3, 6]. The nitric Oxide Synthase (NOS) enzyme is the multi-domain protein in the cytochrome P450 family that produces nitric oxide the smallest signaling molecule known. There

*Corresponding author e-mail: salwahnaser@gmail.com .; (drsalwahnaser@uomustansiriyah.edu.iq).
**Receive Date:** 26 June 2022, **Revise Date:** 03 August 2022, **Accept Date:** 16 August 2022, **First Publish Date:** 16 August 2022
DOI: 10.21608/EJCHEM.2022.147091.6379

are three isoforms of NO synthase: neuronal NOS (nNOS), endothelial NOS (eNOS), inducible NOS (iNOS) in the normal state, and inducible NOS (iNOS) after injury (NOS; EC 1.14.13.39). They all utilize l-arginine [7, 8, 9]. Nitric oxide (NO) is a short-lived free radical gas with an unpaired electron which can be produced immediately in the human body. NO is highly reactive with other molecules like oxygen superoxide, lipids, and proteins via its rapid oxidation into nitrate and nitrite [10, 11, 12]. Pathological NO is considered one of the major mediators in brain damage including hypoxia, ischemic injury, oxidative stress, glutamate neurotoxicity, and neurodegeneration. Increased oxidative and nitrosative stressors, induction of endoplasmic reticulum stress promotion of the mitochondrial permeability transition phase, and activation of mitochondrial apoptotic signaling pathways contribute to neuronal damage when NO levels are high. Therefore, some studies proposed that physiological concentrations of NO are neuroprotective, whereas higher levels are neurotoxic [12, 13, 14, 15]. Vitamin D is a fat-soluble hormone that has a significant role in the homeostasis of calcium, growth, and maintenance of the skeleton. It is believed to play a role in autoimmune diseases like MS and cancer [16, 17, 18]. Vitamin D2 (ergocalciferol) and vitamin D3 (cholecalciferol) are the two types of vitamin D. Ergosterol (pre-vitamin) is a plant source of vitamin D2, whereas 7-dehydrocholesterol, which is mainly synthesized under the skin, is a source of vitamin D3 [19, 20]. In the kidney 25(OH)D3 undergoes a second hydroxylation to form 1,25(OH)2D3 (Calcitriol). This conversion also occurs in the prostate, mammary glands, colon, antigen-presenting cells, macrophages, keratinocytes, and osteoblasts, which all possess the enzyme 1-α-hydroxylase (CYP27B1) responsible for this conversion [21, 22]. The enzyme belongs to the 450-cytochrome family and is classified as a mitochondrial enzyme. The result of translation is a protein with about 508 amino acids, an N-terminal mitochondrial signal sequence and a heme-binding site [23]. Vitamin D has been demonstrated to inhibit the production of inducible nitric acid synthase in microglia; this may influence the balance of inflammatory and anti-inflammatory processes involved in demyelination. Moreover, as a result of vitamin D has a role in the activation of microglial, which promotes myelin debris clearance and then demyelination [24, 25]. Nanotechnology is a branch of science that deals with the creation, manipulation, and application of materials measured in nanometers [26]. Since the beginning of the 20th century the synthesis of gold nanoparticles (AuNPs) has been fascinated by the scientific community due to their unique physical and chemical properties. Because of these special properties, many research groups have tried to use AuNP to solve socially important problems in various fields, including medicine, cosmetology, biology, clinical chemistry, and pharmacology [27, 28]. There are more applications due to the high environmental pollution caused by chemical synthesis. Green synthesis is needed including clean non-toxic and environmentally friendly nanoparticle synthesis methods with sustainable commercial viability [29]. Green synthesis utilizes environmentally friendly non-toxic and safe materials [30] such as plant leaf extracts, bacteria, fungi, and enzymes, to synthesize metal nanoparticles [26, 31]. The present study aims to study the impact of gold nanoparticles in sera of a new diagnosis of multiple sclerosis patients. The activities of the NOS enzyme and CYP27B1 enzyme in the presence and absence of nanoparticles in sera of multiple sclerosis patients were measured through the fabrication and characterization of gold nanoparticles.

## 2. Experimental

**2.1. Materials and Methods:** The raw materials used in this work to prepare gold nanoparticles by chemical reduction are gold tetrachloroauric Acid ($AuCl_4H.3H_2O$) Sigma Aldrich / USA. Tri-Sodium citrate dehydrates/Sigma Aldrich / USA $Na_3C_6H_5O_7.2H_2O$.

### 2.1.1. Preparation of Gold Nanoparticles colloid (AuNPs) by chemical reduction method

Colloidal gold NPs were prepared by chemical reduction method using Trisodium citrate dehydrate ($Na_3C_6H_5O_7.2H_2O$) as a reducing agent. Accordingly, 3mL of 0.02M Trisodium citrate dehydrate was added slowly (drop per second) to 25 mL of 0.001M $HAuCl_4$ under a hot plate with stringing at 70 ˚C for 1. Firstly, the solution turned to dark purple color; then dark red finally became a beet color, after which the stirring was stopped after 1 h. the Colloidal gold NPs were obtained [32, 33].

### 2.1.2. Preparation of Gold Nanoparticles colloid (AuNPs) by green synthesis use Cardamom husks.

Cardamom husks were collected and cleared from dust particles several times with distilled water. The peels were turned into powder after drying in the air overnight, and then crushed in a mortar. 2 gm of the peel powder was boiled in 100 mL of deionized water at 100°C for 30 min. Then, the solution was cooled and filtered. The fresh extract was used to prepare gold nanoparticles according to the procedure: For a typical synthesis, 5 mL cardamom husks extract was added to 25 mL, 0.001M of $HAuCl_4$ for 2 min at 60˚C. The reduction is very rapid and the formation of AuNPs is indicated by a violet shade within 2 min of reaction mixture [34].

### 2.2. Characterization of nanoparticles

Tunneling microscopy, X-ray direction (XRD), Transmission Electron Microscopy (TEM), and Photoluminescence spectroscopy (PL) measurements were used to analyze gold nanoparticles (NPs). The

Debye-relation Scherer's [35] was used to compute the crystallite size.

### 2.3 The cytotoxic effect of gold nanoparticles

**A- Preparation of medium of cancer cell line [36]**

The SH-SY5Y and HDFn cells were suspended in a complete RPMI-1640 medium and allowed to propagate in culture flasks for 48 hrs. In a humidified atmosphere supplemented with 5% $CO_2$ at 37°C. When the cells reached up to 80% confluence the adherent cells were washed twice with PBS solution after removing the growing medium. Two to three mL of trypsin-EDTA solution was added to the flask, and the flask was turned over to cover the monolayer completely with gentle shaking. The flask was incubated at 37°C for 1-2 minutes until the cells were detached from the flask surface. The trypsin was deactivated by adding a complete RPMI-1640 medium followed by distributing cell suspension to other flasks containing fresh complete RPMI medium. Cultured flasks were incubated at 37°C in a 5% atmospheric $CO_2$ incubator. The required cell concentration was obtained using the trypan exclusion cell counting method by mixing 1 volume of cell suspension with 1 volume of trypan blue stain. After 3 min waiting, the cells were counted microscopically using a hemocytometer and applying the formula:

**Total Cell Count mL-1 = Cell count x Dilution Factor (Sample Volume) x $10^4$**

**B- The cytotoxicity test of gold nanoparticles prepared using cardamom husks on the proliferation of the cancerous line**

The cytotoxic effect of the Nanoparticles was performed by using an MTT assay by MTT kit, which contains 1 mL x 10 vials and a solubilization solution 50 mL x 2 bottles. Cells (1 x $10^6$ cells $mL^{-1}$) were grown in 96 flat well micro-titer plates in a final volume of 200 µL complete culture medium per well. The microplate was covered by sterilized parafilm and shacked gently. The plates were incubated at 37°C, 5% $CO_2$ for 48 hrs. After incubation, the medium was removed, and two-fold serial dilutions of the Nanoparticles (12.5, 25, 50, 100, and 200 µM/mL) were added to the wells. Triplicates were used per concentration and the controls (cells treated with serum-free medium). The Plates were incubated at 37°C, 5% $CO_2$ for a selected exposure time (48 hrs.). After exposure, 10 µL of the MTT solution was added to each well. The Plates were further incubated at 37°C, 5% $CO_2$ for 4 hours. The media were carefully removed, and 100 µL of solubilization solution was added per each well for 5 min. At a wavelength of 575 nm, an ELISA reader was used to determine the absorbance. The optical density data were subjected to statistical analysis to determine $IC_{50,}$ the chemical concentration required to cause a 50% loss in cell viability in each cell line.

## 3. Patients and control

### 3.1. Study group

Ninety participants from Iraq's urban and rural areas participated in this study. From April to July 2021, all subjects gave written consent to participate in this study, which was done in the department of multiple sclerosis at Baghdad Teaching Hospital/Medical City. McDonald's criteria were used to diagnose MS, and all patients had RRMS. The RRMS patients were split into two groups. Group I consisted of 30 newly diagnosed RRMS patients aged 19-56 years, while group II involved 30 RRMS patients with treatment (interferon β1b or fingolimod according to medical guidelines) their ages ranging 18-58 years. A total of 30 healthy subjects volunteers served as controls (group III) with age ranged 20-56 years.

### 3.2. Inclusion Criteria

Male and Female inclusive of 18-58 years of age; and multiple sclerosis diagnosis as defined by 2005 revised McDonald criteria.

### 3.3. Exclusion criteria

To eliminate the factors which might affect this study, patients suffering from chronic or acute diseases, such as hypertension, diabetes mellitus, liver or kidney diseases were excluded.

### 3.4. Blood collection

By using 10 mL plastic disposable syringes, ten milliliters of venous blood samples were obtained from each RRMS patient and control, the sample was allowed to clot for 30 minutes at 25°C in a Gel tube. After centrifugation at 1500 xg for 10 minutes, the serum was collected and stored at -20°C until NOS and CYP27B1enzyme analysis. Patients with chronic or acute disorders such as diabetes, hypertension, renal, or liver disease were not included in this study.

### 3.5. Laboratory analysis

Serum levels of NOS and CYP27B1 enzyme were assayed by a double-antibody sandwich Enzyme-Linked Immunosorbent Assay (ELISA) kits obtained from (Melsin Medical Co., Limited, China) according to the provided assay procedure. Each assay was calibrated using its standard curve following the manufacturer's instructions and using the instruments (Reader and Washer, HUMAN, Germany).

### 3.6. Determination of human serum NOS and CYP27B1 level by ELISA kit

The level of human NOS enzymes and CYP27B1 enzyme was determined in the presence and absence of AuNPs in this assay; patients who used a drug were excluded (n=30).

Preparation of serum sample: an aliquot serum sample (10µL) from each patient (n=30) was pipetted into a tube to make the final volume 300 µL to prepare the serum mixture sample.
The effect of NPs on NOS and CYP27B1 activity was investigated using ELISA technique. Standards and samples are added in duplicate to the Microelisa Stripplate. The 40 µL dilution buffer and 10mL of pool sample mixture were added to the well at the end of 5, 10, 15, 20, 25, 30 minutes to form a total volume of 50 µL (duplicated).

### 3.7. Statistical Analysis

The study results are presented as mean ±standard deviation (SD) and statistically analyzed using the social sciences (SPSS) statistics version 25 application. The difference between groups was measured using one-way variance analysis (ANOVA).

## 4. Results and Discussion

The bio synthesis of Au NPs in this study was done by reducing the gold aqueous solution ($HAuCl_4.3H_2O$) using Cardamom husks acts as both the reducing and stabilizing agent.

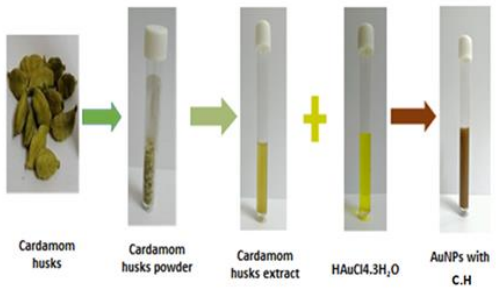


**Fig. 1:** The change in color indicating the synthesis of AuNPs with Cardamom husks.

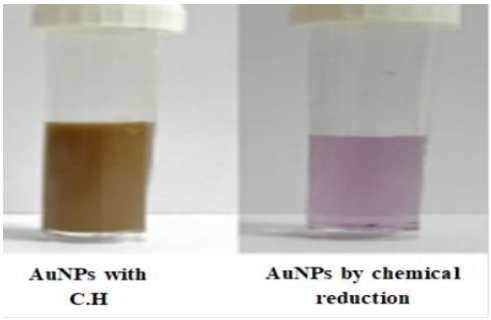


**Fig. 2:** The change in color indicating the synthesis of AuNPs with Cardamom husks and AuNPs by chemical reduction.

Figures 3 and 4 show the XRD patterns of the AuNPs. All of the peaks match Au polycrystalline phase (JCPDS No. 00-004-0784), and no peaks of impurities were detected, indicating that the Au nanoparticles were pure and well crystallized. The XRD patterns of Au contained four main peaks at 2 theta 38.29◦, 44.49◦, 64.84◦, and 77.79◦, which correspond to the (111), (200), (220), and (311), respectively, Scherer's equation [37, 38]. Was used to calculate the crystallite size, and the results are shown in Table 1.

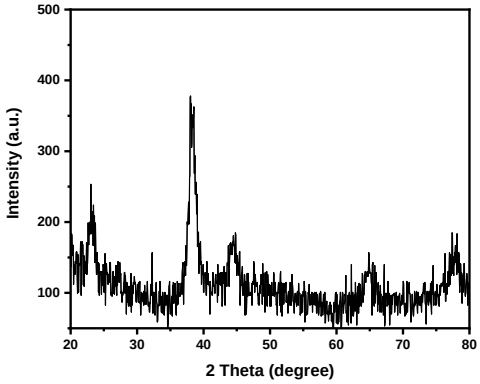


**Fig. 3:** X-ray diffract gram of the synthesized Au NPs with a simple chemical reaction.

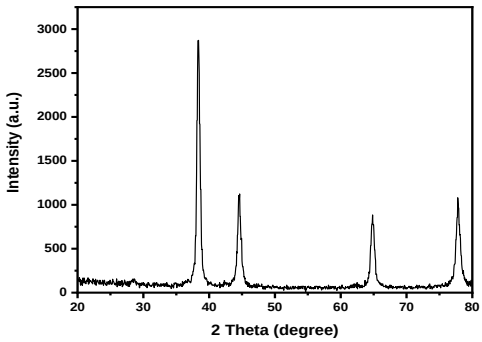


**Fig. 4:** XRD spectra for AuNPs forms using Cardamom husks.

The morphology and particle size of AuNPs have been determined by TEM. The mean particle size and distribution are determined randomly on the TEM images of the samples, as shown in Figures 5 and 6. TEM images proved that all the prepared gold nanoparticles are spherical and without any aggregations. It was subjected to synthesis mechanics from the bottom up. The dimensions of synthesized nanoparticles were within the nanoscale (all measurements less than 100 nm), which indicated the type of the nano being nanoparticles and the zero dimension (0D). The particle size of all nanoparticles obtained from TEM studies was in close agreement with the X-ray size obtained from Scherrer's equation using X-ray line broadening studies.

Figures 7 and 8 exhibits the Photoluminescence spectroscopy spectrum for samples at room temperature to measure the emission energy gap using a solid-state photoluminescent spectrum for preparing its emissions. Figures 7 and 8 are Photoluminescence

analysis showed two emission peaks for Au NPs first higher intensity emission in the violet region at 370 nm that peak was due to the Ultraviolet-emission band will be described mainly through near band edge emission (NBE) transition including the wide bandgap of Au nanoparticles, the second faint visible emission peak at 460 nm with blue emission reveals that the surface Plasmon resonance is a recombination of free excitons by the exciton-exciton collision event [39].

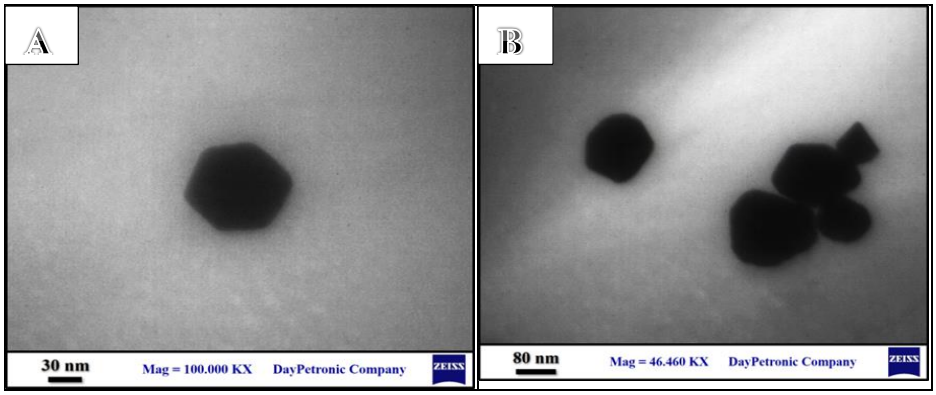


**Fig. 6:** TEM images of Au NPs Cardamom husks; A- with 30 nm, B- with 80 nm.

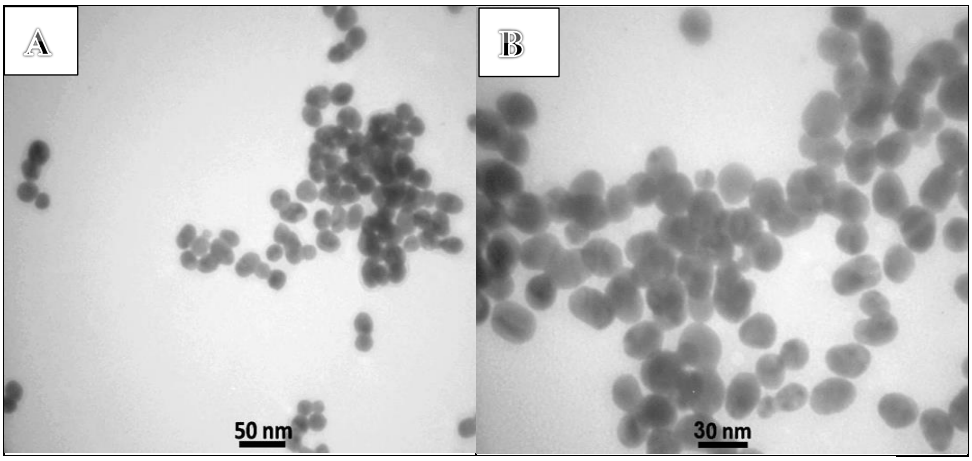


**Fig. 5:** TEM images of Au NPs with simple chemical reduction; A- with 50 nm, B- with 30nm.

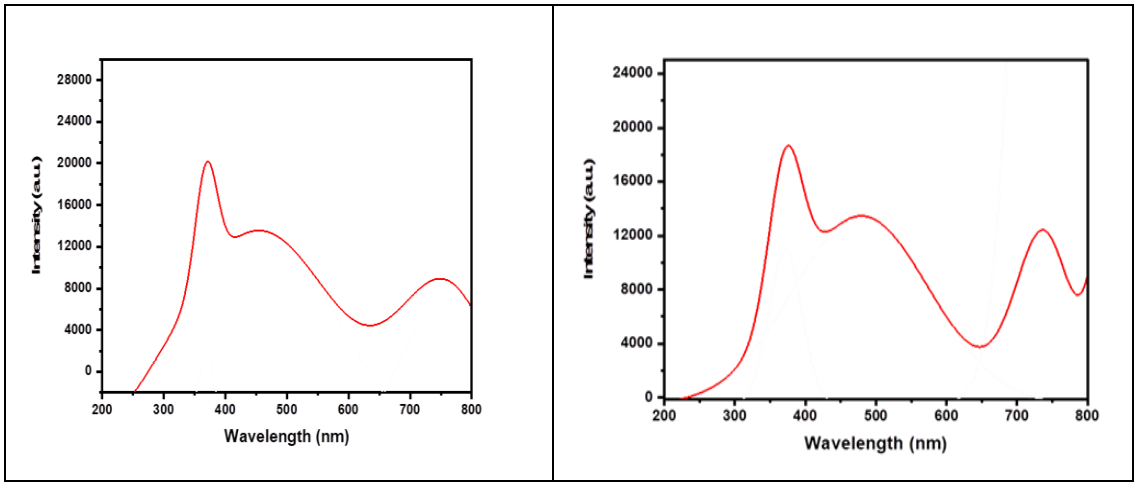


**Fig. 7:** The PL analysis of Au NPs with simple chemical reaction.

**Fig.8:** The PL analysis of Au NPs using Cardamom husks.

**Table 1: Summery of X-RAY characterization for AuNPs**

| (hkL)planes | 2 theta (deg.) | beta | cos theta (rad) | D nm |
|---|---|---|---|---|
| 111 | 38.29 | 0.3936 | 0.944 | 21.26 |
| 200 | 44.49 | 0.2952 | 0.925 | 28.938 |
| 220 | 64.84 | 0.3444 | 0.843 | 27.225 |
| 311 | 77.79 | 0.246 | 0.776 | 41.380 |

### 4.1 Cytotoxic effect of gold nanoparticles on Tumour Cell Line

To study the toxicity of nanoparticles prepared from chemical reduction and green synthesis, the nanoparticles were investigated in vitro against the Human Neuroblastoma Cell Line (SH-SY5Y) and the Human dermal fibroblasts (HDFn). The effect of the nanoparticles on cell growth was determined by using the MTT assay after treatment of the cell line with different concentrations (12.5, 25, 50, 100, and 200 µM/mL) for 48 hours. Figure 9 shows the effect of the test compounds on cell viability. Table 2 shows the calculated inhibition percentage of cell growth.

The results indicated that the AuNPs with Cardamom husks and AuNPs by chemical reduction cause strong cytotoxicity in Table 2. The results showed the $IC_{50}$ calculated from compounds treatment against SH-SY5Y was found to be the highest cytotoxic activity than that calculated for HDFn cells. However, the $IC_{50}$ calculated from AuNPs with C.H treatment against SH-SY5Y was found to be the highest cytotoxic activity at 43.0 µM, demonstrating a high level of selectivity for the human neuroblastoma cell line, indicating that it could be used as a potential anticancer drug. Human neuroblastoma cell line (SH-SY5Y) but weak and moderate cytotoxicity on standard cell lines (HDFn). AuNPs with Cardamom husks shows higher inhibition than AuNPs by chemical reduction. To improve the higher cytotoxicity level AuNPs with H.C have different levels of inhibitory effect on cancer cell growth. The inhibition of SH-SY5Y cells was highly significant, P = 0.0001 increased by increasing compound concentration compared with normal HDFn cells inhibition, especially at 200 µM/mL. The maximum inhibition rate at 46.644±3.478% was observed at 200 µM/mL for AuNPs with Cardamom husks. The $IC_{50}$ value of this compounds ware explained in Figure 9 and determined by using different concentrations.

### 4.2 Application study (in vitro) of Nanoparticles on human newly diagnosed patients Multiple Sclerosis.

Nanomedicine is a new growing discipline of nanotechnology that created a new bridge between nanotechnology and biotechnology, dubbed the "nano-bio interface." Nanomaterials provide considerable promise for new medical diagnostic possibilities due to their innovative physicochemical properties [40].

In this part, the activity of NOS and CYP27B1 enzyme was investigated in the presence and absence of AuNPs with Cardamom husks and AuNPs by chemical reduction.

**Table 2: Effect of the Nanoparticles on the SH-SY5Y and HDFn cell proliferation at different concentrations for 48 hours P ≤ 0.0001, (*) Non-Significant, Results are presented as means ± SD, N=3**

| Test Compound | | | AuNPs with C.H Mean ± SD | AuNPs by chemical reduction Mean ± SD |
|---|---|---|---|---|
| Cell Growth Inhibition (%) ± SD | 12.5 µM/mL | SH-SY5Y | 3.048±1.142 | 13.117±4.558 |
| | | HDFn | 4.205±0.876 | 3.048±1.752 |
| | 25 µM/mL | SH-SY5Y | 15.394±1.252* | 35.069±3.282* |
| | | HDFn | 4.282±1.514 | 9.645±1.642 |
| | 50 µM/mL | SH-SY5Y | 27.932±3.093* | 47.145±2.974* |
| | | HDFn | 9.722±3.720 | 25.579±1.518 |
| | 100 µM/mL | SH-SY5Y | 39.043±0.928* | 54.63±4.206* |
| | | HDFn | 12.076±3.579 | 36.497±2.589 |
| | 200 µM/mL | SH-SY5Y | 46.644±3.478* | 64.545±3.513* |
| | | HDFn | 19.637±2.275 | 49.691±4.477 |

SH-SY5Y: Human Neuroblastoma Cell Line; HDFn: Human Normal dermal fibroblasts cell line; C.H: Cardamom husks; The Mean ± SE of different concentration (12.5, 25, 50, 100 and 200 µM/mL) of NPs on cell line after 48 hrs.

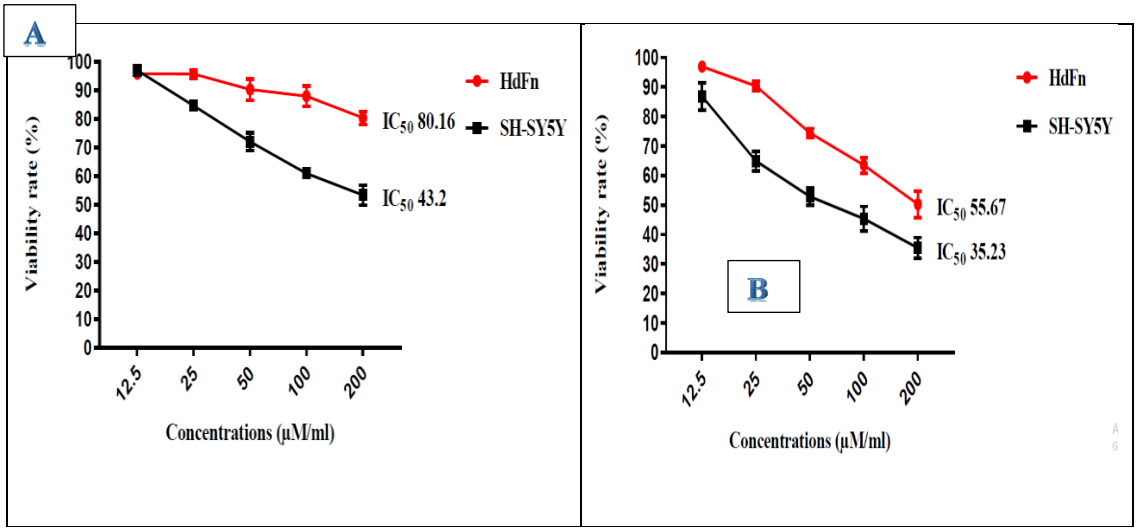


**Fig. 9:** Cell survival curve (mean ± SD %) of SH-SY5Y cells and HDFn after treatment with Nanoparticles using MTT assay at 37ºC, 5% $CO_2$ for 48 hours, $p \leq 0.0001$, SD: Standard Deviation, N=3; A: gold nanoparticles with cardamom husks; B: gold nanoparticles by the chemical method.

The effects of presence AuNPs with Cardamom husks and AuNPs by chemical reduction on the levels of NOS in sera of patients with MS showed inhibition effect (48.51%, 25.63%), respectively, in Figure 10 by using the same kit conditions mentioned in experimental work (3.6) with adding 10µL of NPs. The interaction between proteins and AuNPs depends upon three separate but dependent phenomena: a) Ionic attraction between the negatively charged gold and the positively charged proteins; b) Hydrophobic attraction between the Antibody and the gold surface; c) Dative binding between the gold conducting electrons and sulfur atoms which may occur with amino acids of the proteins [41].

While we found in the study that AuNPs with Cardamom husks and AuNPs by chemical reduction not demonstrated effects inhibited on the binding between anti- CYP27B1antibody and antigen CYP27B1 level in pool sera of MS patients, as shown in Figures 11.

The inhibition in the activity of NOS and CYP27B1 was calculated in the presence of nanoparticles for detecting the optimum using the following equation:

$$\text{Inhibition}\,(\%) = \left(\frac{Ci - Cf}{Ci}\right) \times 100 \quad \ldots\ldots\ldots\ldots\ldots (3\text{-}3)$$

Were Ci is the activity of NOS and CYP27B1, and Cf the activity in presence of AuNPs compounds.

Various incubation times of the Antigen-Antibody reaction were evaluated. In serum at the incubation temperature of 37ºC We found increasing in the binding for NOS with an increased incubation time the maximum time is 30 min., as seen in Figure 12. We found the non-significant effect of optimum incubation time it does not appear on the CYP27B1 level in the pooling of sera sample (N-RRMS) in MS, as shown in figure 12.

Other results showed that oral delivery of gold nanocrystals improved motor functions of cuprizone-treated mice. Gold nanocrystal treatment of oligodendrocyte precursor cells in culture resulted in oligodendrocyte maturation and expression of myelin differentiation markers [42].

Also, the goal of this study [43] sought to demonstrate the improving effect of gold nanoparticles (GNPs) on the demyelinating effect of injection of L-arginine in the animal model as a progenitor of pro-inflammatory factor (nitric oxide) in the brain results show that L-arginine caused increased density of neurons in the target area of experimental animals in comparison with that of the control groups.

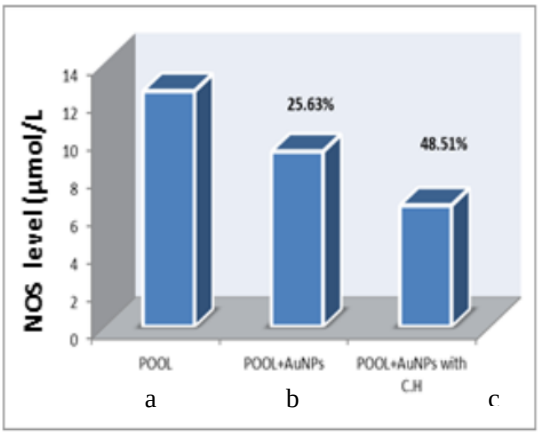


Fig. 10: The NOS (µmol/L) levels in sera of (a) pool N-RRMS, (b) pool N-RRMS and AuNPs by chemical reduction, (c) pool N-RRMS and AuNPs with Cardamom husks.

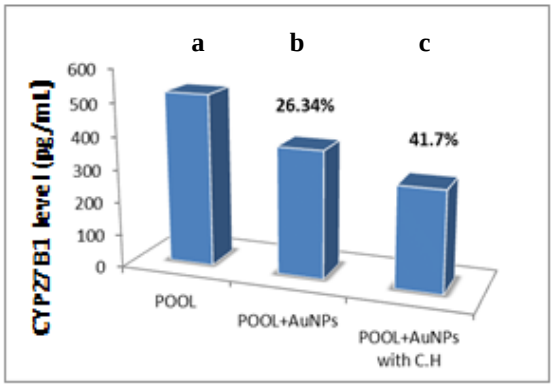


Fig. 11: The CYP27B1 (pg/mL)level in sera of (a) pool N-RRMS, (b) pool N-RRMS and AuNPs by chemical reduction, (c) pool N-RRMS and AuNPs with Cardamom husks.

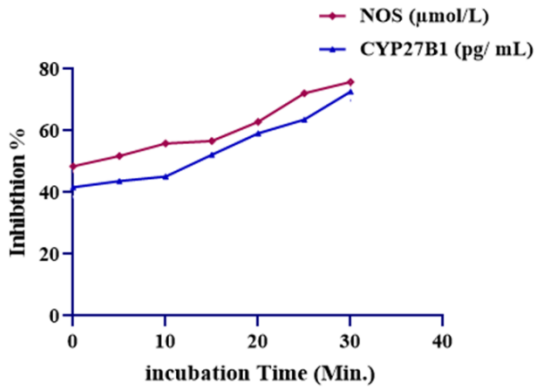


Fig. 12: Line chart of NOS and CYP27B1 levels incubated with AuNPs. t0: the NOS and CYP27B1 level of N-RRMS patient in absence of AuNPs with Cardamom husks. The t5, t10, t15, t20, t25, t30 NOS and CYP27B1 level in presence of AuNPs with Cardamom husks in different incubation time.

Other researchers have also made similar conclusions about the MS since they have reported that its diagnosis was even improved with the application of very small superparamagnetic iron oxide particles, which showed a characteristic accumulation in the inflammatory lesions [44]

The work aimed to study the effects of NPs on the levels of NOS and CYP27B1activity in the serum of newly diagnosed MS patients. Also, the study characterized the binding between the anti-CYP2D6, CYP27B1and NOS antibody with its antigen in serum N-RRMS of NPs the current study of AuNPs could be a stepping stone for future work to improve the binding between the vitamin D and its receptors inside the body and could be used to improve and modify a competitive ELISA method.

## 7. Conclusion

Gold nanoparticles were synthesized by the chemical reduction method and green synthesis as spherical shapes with small diameters of up to 20 nm and without agglomerations. The result indicated that AuNPs had inhibition effects on NOS while not demonstrating effects that inhibited the CYP27B1activities. So, these nanoparticles may play an essential role in drug delivery for treating multiple sclerosis. Gold nanoparticles with cardamom husks are more effective inhibitors than AuNPs by chemical reduction of the activity of NOS.

## 8. Conflicts of interest

There are no conflicts to declare.

## 9. Acknowledgments

The Iraqi Ministry of Higher Education and Scientific Research, as well as Mustansiriyah University, College of Science, and Department of Chemistry, have provided support.

## 10. References

[1] F. Faraji, M. Hashemi, A. Ghiasabadi, S. Davoudian, A. Ganji, & G. Mosayebi, (2019).“Combination therapy with interferon beta-1a and sesame oil in multiple sclerosis”. Complementary therapies in medicine, 45, pp. 275-279. doi: 10.1016/j.ctim.2019.04.010.

[2] R. Dobson, & G. Giovannoni, (2019). “Multiple sclerosis–a review”. European journal of neurology, 26(1), pp. 27-40.

[3] X. Li, J. Yuan, J. Han, and W. Hu, (2020). “Serum levels of homocysteine, vitamin B12 and folate in patients with multiple sclerosis: an updated meta-analysis”. International journal of medical sciences, 17(6), pp. 751–761. doi: 10.7150/ijms.42058.

[4] V. Văcăraș, V. Văcăraș, C. Nistor, D. Văcăraș, A. N. Opre, P. Blaga, & D. F. Mureșanu, (2020). “The influence of depression and anxiety on neurological disability in multiple sclerosis patients”. Behavioural Neurology, 2020. doi: 10.1155/2020/6738645.

[5] C. Silveira, R. Guedes, D. Maia, R. Curral, and R. Coelho, (2019). Neuropsychiatric symptoms of multiple sclerosis: state of the art. Psychiatry Investigation, 16(12), p. 877.

[6] L. Pan, Y. Yin, J. Chen, Z. Ma, Y. Chen, X. Deng, H. T. Zhang, H. Leng, & K. Wu, (2019). Homocysteine, vitamin B12, and folate levels in patients with multiple sclerosis in Chinese population: A case-control study and meta-analysis. Multiple Sclerosis and Related Disorders, 36(June). doi: 10.1016/j.msard.2019.101395.

[7] S. A. Sonar and G. Lal, (2019). ‘The iNOS activity during an immune response controls the CNS pathology in experimental autoimmune encephalomyelitis’, Frontiers in

Immunology, 10(APR). doi: 10.3389/fimmu.2019.00710.

[8] R. Minhas, Y. Bansal, and G. Bansal, (2020), 'Inducible nitric oxide synthase inhibitors: A comprehensive update', Medicinal Research Reviews, 40(3), pp. 823–855. doi: 10.1002/med.21636.

[9] J. A. G. Agúndez, E. García-Martín, C. Rodríguez, J. Benito-León, J. Millán-Pascual, M. Díaz-Sánchez, P. Calleja, L. Turpín-Fenoll, H. Alonso-Navarro, E. García-Albea, J. F. Plaza-Nieto, & J. Félix Jiménez-Jiménez, (2020) 'Endothelial nitric oxide synthase (NOS3) rs2070744 polymorphism and risk for multiple sclerosis', Journal of Neural Transmission, 127(8), pp. 1167–1175. doi: 10.1007/s00702-020-02211-0.

[10] M. Lan, X. Tang, J. Zhang, and Z. Yao, (2018). Insights in pathogenesis of multiple sclerosis: nitric oxide may induce mitochondrial dysfunction of oligodendrocytes. Reviews in the Neurosciences, 29(1), pp. 39–53.

[11] M. Rizzi, D. Radovanovic, A. Airoldi, A. Cristiano, F. Frassanito, P. Gaboardi, & P. Santus, (2019). Rationale underlying the measurement of fractional exhaled nitric oxide in systemic sclerosis patients. Clin. Exp. Rheumatol, 37, pp. 125-132.

[12] P. Picón-Pagès, J. Garcia-Buendia, and F. J. Muñoz, (2019) 'Functions and dysfunctions of nitric oxide in brain', Biochimica et Biophysica Acta - Molecular Basis of Disease, 1865(8), pp. 1949–1967. doi: 10.1016/j.bbadis.2018.11.007.

[13] M. Lan, X. Tang, J. Zhang, and Z. Yao, "Insights in pathogenesis of multiple sclerosis: Nitric oxide may induce mitochondrial dysfunction of oligodendrocytes," Rev. Neurosci., vol. 29, no. 1, pp. 39–53, 2017, doi: 10.1515/revneuro-2017-0033.

[14] U. Förstermann and W. C. Sessa, (2012) 'Nitric oxide synthases: Regulation and function', European Heart Journal, 33(7), pp. 1–13. doi: 10.1093/eurheartj/ehr304.

[15] C. M. Chong, N. Ai, M. Ke, Y. Tan, Z. Huang, Y. Li, & H. Su, (2018). Roles of nitric oxide synthase isoforms in neurogenesis. Molecular neurobiology, 55(3), pp. 2645-2652.

[16] N. Hu and H. Zhang, (2018) 'CYP24A1 depletion facilitates the antitumor effect of vitamin D3 on thyroid cancer cells', Experimental and Therapeutic Medicine, 16(4), pp. 2821–2830.

[17] C. Scazzone, L. Agnello, G. Bivona, B. Lo Sasso, and M. Ciaccio, (2018). Association of CYP2R1 rs10766197 with MS risk and disease progression. Journal of neuroscience research, 96(2), pp. 297-304.

[18] C. Wang, Z. Zeng, B. Wang, and S. Guo, (2018). Lower 25-Hydroxyvitamin D is associated with higher relapse risk in patients with relapsing-remitting multiple sclerosis. The journal of nutrition, health & aging, 22(1), pp. 38-43.

[19] Á. Gil, J. Plaza-Diaz, and M. D. María, (2018). Vitamin D: classic and novel actions. Annals of Nutrition and Metabolism, 72(2), 87-95.

[20] V. Pytel, J. A. Matías-Guiu, L. Torre-Fuentes, P. Montero-Escribano, P. Maietta, J. Botet, & J. Matías-Guiu, (2019). Exonic variants of genes related to the vitamin D signaling pathway in the families of familial multiple sclerosis using whole-exome next generation sequencing. Brain and behavior, 9(4), p.e01272.

[21] S. J. Newberry, M. Chung, P. G. Shekelle, M. S. Booth, J. L. Liu, A. R. Maher, A. Motala, M. Cui, T. Perry, R. Shanman, & E. M. Balk, (2014). Vitamin D and calcium: a systematic review of health outcomes (update). Evidence report/technology assessment, (217), pp.1-929.

[22] Yang, P., & Ma, Y. (2021). Recent advances of vitamin D in immune, reproduction, performance for pig: A review. Animal Health Research Reviews, pp. 1-11. doi: 10.1017/S1466252321000049.

[23] M. Latacz, J. Snarska, E. Kostyra, E. Fiedorowicz, H. F. Savelkoul, R. Grzybowski, & A. Cieślińska, (2020). Single nucleotide polymorphisms in 25-hydroxyvitamin D3 1-alpha-hydroxylase (CYP27B1) gene: the risk of malignant tumors and other chronic diseases. Nutrients, 12(3), 801. doi: 10.3390/nu12030801.

[24] (2017) 'Loss of tuberous sclerosis complex1 in adult oligodendrocyte progenitor cells enhances axon remyelination and increases myelin thickness after a focal demyelination', Journal of Neuroscience, 37(31), pp. 7534–7546.

[25] H. Katsuki, (2021). Nuclear receptors of NR1 and NR4 subfamilies in the regulation of microglial functions and pathology. Pharmacology Research & Perspectives, 9(6), e00766.

[26] I. F. Ascar, S. B. Al-A'Araji, and A. F. Alshanon, (2019) 'Cytotoxicity and antioxidant effect of ginger gold nanoparticles on thyroid carcinoma cells', Journal of Pharmaceutical Sciences and Research, 11(3), pp. 1044–1051.

[27] A. Dzimitrowicz, P. Jamroz, I. Sergiel, T. Kozlecki, P. Pohl, and others, (2019) 'Preparation and characterization of gold

nanoparticles prepared with aqueous extracts of Lamiaceae plants and the effect of follow-up treatment with atmospheric pressure glow microdischarge', Arabian Journal of Chemistry, 12(8), pp. 4118–4130.

[28] J. Qiao and L. Qi, (2021). Recent progress in plant-gold nanoparticles fabrication methods and bio-applications. Talanta, 223, 121396.

[29] R. T. Kapoor, M. R. Salvadori, M. Rafatullah, M. R. Siddiqui, M. A. Khan, and S. A. Alshareef, (2021). Exploration of microbial factories for synthesis of nanoparticles–a sustainable approach for bioremediation of environmental contaminants. Frontiers in Microbiology, 12, 658294.

[30] M. W. Ullah, S. Manan, W. A. Khattak, A. Shahzad, M. Ul-Islam, and G. Yang, (2020). Biotemplate-mediated green synthesis and applications of nanomaterials. Current Pharmaceutical Design, 26(45), 5819-5836.

[31] M. Ali, T. Ahmed, W. Wu, A. Hossain, R. Hafeez, M. Islam M. Masum, , Y. Wang, Q. An, G. Sun, & B. Li, (2020). Advancements in plant and microbe-based synthesis of metallic nanoparticles and their antimicrobial activity against plant pathogens. Nanomaterials, 10(6), 1146.

[32] T. A. Ivandini, M. S. P. Luhur, M. Khalil, and Y. Einaga, (2021). Modification of boron-doped diamond electrodes with gold–palladium nanoparticles for an oxygen sensor. Analyst, 146(9), 2842-2850. doi: 10.1039/d0an02414g.

[33] Y. Duan, W. Wu, Q. Zhao, S. Liu, H. Liu, M. Huang, & Z. Wang, (2020). Enzyme-antibody-modified gold nanoparticle probes for the ultrasensitive detection of nucleocapsid protein in SFTSV. International Journal of Environmental Research and Public Health, 17(12), 4427.

[34] A. Rajan, A. R. Rajan, and D. Philip, (2017) 'Elettaria cardamomum seed mediated rapid synthesis of gold nanoparticles and its biological activities', OpenNano, 2(November 2016), pp. 1–8. doi: 10.1016/j.onano.2016.11.002.

[Yadav, J. (2018) 'Synthesis and Characterization of Gold Nanoparticles', (April), pp. 220–230.

[36] R. I. Freshney, "(2005). Laboratory design and layout. Culture of Animal Cells: a manual of basic technique. doi: 10.1002/9780471747598.

[37] O. H. Abdullah and A. M. Mohammed, (2020) 'Green synthesis of aunps from the leaf extract of prosopis farcta for antibacterial and anti-cancer applications', Digest Journal of Nanomaterials and Biostructures, 15(3), pp. 943–951.

[38] M. R. Bindhu, P. Saranya, M. Sheeba, C. Vijilvani, T. S. Rejiniemon, A. M. Al-Mohaimeed, & M. S. Elshikh, (2021). Functionalization of gold nanoparticles by β-cyclodextrin as a probe for the detection of heavy metals in water and photocatalytic degradation of textile dye. Environmental Research, 201, 111628, doi: 10.1016/j.envres.2021.111628.

[39] Y. Y. Cai, J. G. Liu, L. J. Tauzin, D. Huang, E. Sung, H. Zhang, A. Joplin, W. S. Chang, P. Nordlander, and S. Link, S. (2018) 'Photoluminescence of Gold Nanorods: Purcell Effect Enhanced Emission from Hot Carriers', ACS Nano, 12(2), pp. 976–985. doi: 10.1021/acsnano.7b07402.

[40] N. A.-A. Aboud, W. M. S. Alkayat, D. H. Hussain, and A. M. Rheima, (2020) 'A comparative study of ZnO, CuO and a binary mixture of $ZnO^0$. 5-$CuO^0$. 5 with nano-dye on the efficiency of the dye-sensitized solar cell', in Journal of Physics: Conference Series, p. 12094.

[41] A. Ambrosi, F. Airo, and A. Merkoçi, (2010) 'Enhanced gold nanoparticle based ELISA for a breast cancer biomarker', Analytical chemistry, 82(3), pp. 1151–1156.

[42] A. P. Robinson, J. Z. Zhang, H. E. Titus, M. Karl, M. Merzliakov, A. R. Dorfman, & S. D. Miller. (2020). Nanocatalytic activity of clean-surfaced, faceted nanocrystalline gold enhances remyelination in animal models of multiple sclerosis. Scientific reports, 10(1), 1-16.

[43] M. Khosravi, M. Karami, M. J. Nadoushan, and A. Hajnorouzi, (2019). Myelin enhancement of Multiple sclerosis model with gold nanoparticles into the corpus callosum. Nanomedicine Journal, 6(3).

[44] J. M. Millward, J. Schnorr, M. Taupitz, S. Wagner, J. T. Wuerfel, and C. Infante-Duarte, (2013). Iron oxide magnetic nanoparticles highlight early involvement of the choroid plexus in central nervous system inflammation.